Exploiting Magnetic Resonance Angiography Imaging Improves Model Estimation of BOLD Signal

Zhenghui Hu[1]*, **Cong Liu**[1], **Pengcheng Shi**[2,3], **Huafeng Liu**[1]*

1 State Key Laboratory of Modern Optical Instrumentation, Zhejiang University, Hangzhou, China, 2 B. Thomas Golisano College of Computing and Information Sciences, Rochester Institute of Technology, Rochester, New York, United States of America, 3 University of Rochester Medical Center, Rochester, New York, United States of America

Abstract

The change of BOLD signal relies heavily upon the resting blood volume fraction (V_0) associated with regional vasculature. However, existing hemodynamic data assimilation studies pretermit such concern. They simply assign the value in a physiologically plausible range to get over ill-conditioning of the assimilation problem and fail to explore actual V_0. Such performance might lead to unreliable model estimation. In this work, we present the first exploration of the influence of V_0 on fMRI data assimilation, where actual V_0 within a given cortical area was calibrated by an MR angiography experiment and then was augmented into the assimilation scheme. We have investigated the impact of V_0 on single-region data assimilation and multi-region data assimilation (dynamic cause modeling, DCM) in a classical flashing checkerboard experiment. Results show that the employment of an assumed V_0 in fMRI data assimilation is only suitable for fMRI signal reconstruction and activation detection grounded on this signal, and not suitable for estimation of unobserved states and effective connectivity study. We thereby argue that introducing physically realistic V_0 in the assimilation process may provide more reliable estimation of physiological information, which contributes to a better understanding of the underlying hemodynamic processes. Such an effort is valuable and should be well appreciated.

Competing Interests: The authors have declared that no competing interests exist.

* E-mail: zhenghui@zju.edu.cn (ZH); liuhf@zju.edu.cn (HL)

Introduction

In 1998, Buxton and his colleagues introduced their celebrated hemodynamic model, Balloon model [1]. The comprehensive biophysical model of hemodynamic modulation describes the coupling dynamics from neural activity to observed blood oxygen level dependent (BOLD) signal [1,2]. It comprises the coupling mechanism of manifold physiological variables, blood flow (f), blood volume (v), and deoxyhemoglobin content (q), during brain activation. This model then has been extended to include the effects of external inputs on blood flow inducing signal by Friston et al [3]. Since its inception, there is a growing interest in assimilating such a model with given sets of fMRI measurements in order to infer physiological parameters and associated states [4–9], constrain the activation detection process with classic statistics techniques [10,11], and extrapolate to similar systems and/or different driving conditions [12–16]. Although these works greatly enhance our understanding of the neural systems that mediate specific cognitive processes, they are still kind of problematic in offering reliable inference on the hemodynamic system behaviors.

The query on reliability of estimation primarily comes from the assumption about resting blood volume fraction (V_0) in the assimilation procedure. It has long been noted that BOLD contrast is highly weighted by venous blood content. The change of signal intensity in given region thereby depends heavily on local vessel geometry including capillaries and large veins. The evaluation of model structure also indicates that V_0 is a leading influence mechanism in driving the model output uncertainty [17]. However, This parameter can not be identified along with other model parameters simultaneously due to the ill-conditioning of the inverse problem. All studies so far have engaged a physiological plausible value $V_0 = 0.02$ in region of interest (ROI) [3–9,18] or throughout the whole brain [10,11] to dispel the ill-conditioning problem, instead of investigating actual V_0. When a voxel includes only brain tissue, the assumption $V_0 = 0.02$ is reasonable [3,19]. When a voxel is mostly or totally occupied by a vessel or vessels, however, the value might typically be above 0.6 [20]. On the other hand, these voxels that contain large blood content are always more likely to show significant BOLD activation due to the nature of fMRI technique. In this situation, the employment of unrealistic V_0 value in data assimilation might produce unreliable model estimation, far straying from physiological reality. The effort of incorporating actual vascular information of voxels into the fMRI data assimilation therefore should be well appreciated.

In this study, we presented the first attempt to exploit actual resting blood volume fraction in assimilation procedure. The actual V_0 is derived from the segmentation of the vein in the MR angiography (MRA), then augmented into the existing assimilation schemes. As physical realistic V_0 is adopted in assimilation process, more reasonable inference about hemodynamic behavior can thus

be expected. We will illustrate the efficacy of the combinative approach on single-region data assimilation and multi-region data assimilation.

This paper is organized as follows. We first simply review the hemodynamic Balloon model and its formulation that forms the basis of data assimilation, then describe the derivation of V_0 from MRA images. The impacts of actual V_0 on states forecast and parameter estimation are presented in terms of data assimilation and dynamic causal models subsequently.

Methods

Hemodynamic Balloon Model

The original hemodynamic Balloon model consists of three subsystem linkings: (1) neural activity to changes in flow; (2) changes in flow to changes in blood volume and venous outflow; (3) changes in flow, volume and oxygen extraction fraction to changes in deoxyhemoglobin (dHb). It describes the dynamic intertwinement between the blood flow f, the blood venous volume v and the veins dHb content q, which can be given as the following [1,3]:

$$\begin{cases} \ddot{f} = \epsilon u(t) - \dfrac{\dot{f}}{\tau_s} - \dfrac{f-1}{\tau_f} \\ \dot{v} = \dfrac{1}{\tau_0}(f - v^{1/\alpha}) \\ \dot{q} = \dfrac{1}{\tau_0}(f \dfrac{1-(1-E_0)^{1/f}}{E_0} - v^{1/\alpha}\dfrac{q}{v}) \end{cases} \quad (1)$$

where ϵ is neuronal efficacy; $u(t)$ is the neuronal input; τ_s reflects signal decay; τ_f is the feedback autoregulation time constant; τ_0 is the transit time; α is the stiffness parameter; and E_0 denotes the resting oxygen extraction fraction. All variables are expressed in normalized form, relative to resting values. The input-state-output system is represented by nonlinear equations of a series of physiological states. Equation (1) has a second-order time derivative, and we can write this system as a set of four first-order ordinary differential equations (ODEs) by introducing a new variable $s=\dot{f}$. Although the Balloon model is enhanced somehow afterwards [21–23], the model structure analysis shows that the original model is sufficient to account for the hemodynamic response in sparse, noisy fMRI measurement [11,17].

Furthermore, the BOLD observation can be expressed as:

$$\begin{cases} y(t) = V_0(k_1(1-q) + k_2(1-\dfrac{q}{v}) + k_3(1-v)), \\ k_1 = 7E_0, \quad k_2 = 2, \quad k_3 = 2E_0 - 0.2, \end{cases} \quad (2)$$

appropriate for a 1.5 Tesla magnet [1]. V_0 is the resting blood volume fraction, which may vary across brain regions and across subjects. The model architecture is summarised in Figure 1.

For any given combination of parameters $\mathbf{q} = \{\epsilon, \tau_s, \tau_f, \tau_0, \alpha, E_0, V_0\}$ and neuronal inputs u, equations (1) and (2) produce a predicted BOLD response. They form the basis for fMRI data assimilation from the measured dataset. Note that parameter V_0 can not be identified along with other parameters simultaneously, but only their product is admitted. Up to now, all existing efforts have circumvented the ill-conditioning nature by imposing a physiological plausible value $V_0 = 0.02$ [4–8,10–16]. However, the usage of this parameter value is expedient so that the assimilation problem can be solved. Since the change in the BOLD signal depends heavily on V_0, unrealistic V_0 may lead to unreliable model parameter estimation. In addition, the stiffness parameter α shows a marginal influence to the system output variance, and it can be fixed within its physiological reasonable range ($\alpha = 0.33$ here) without significant loss of information in data assimilation processing [8,10,11,17].

Derivation of V_0 from MR Angiography Image

In hemodynamic model, V_0 is defined as the venous volume of blood present in a voxel. It represents the ratio occupied vessels with sizes ranging from capillaries to large veins that all contribute to fMRI measurements in the area [1,2]. Typical resting value in brain tissue which only contains capillaries is around 2 per cent. When a vessel or vessels are present in a voxel, local blood volume will dramatically rise. The value in large vessel region is typically above 0.6. The presence of large vessel is expected to make V_0 inhomogeneous. Fortunately, large blood vessel are accessible by MR angiography (MRA) imaging.

Consider that V_0 in a voxel consists of two different derivative components, constant tissue blood volume component V_s and varied large blood vessels component V_l:
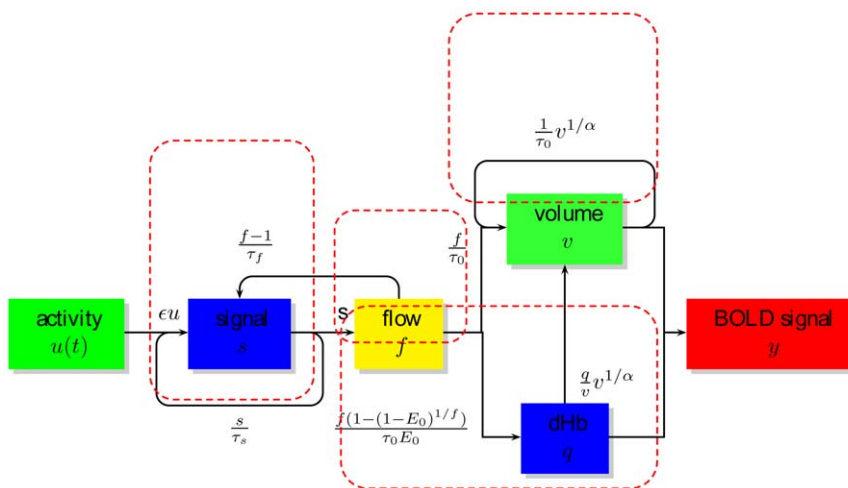
$$V_0 = V_s + V_l \quad (3)$$

Figure 1. Schematic illustration of the hemodynamic Balloon model.
doi:10.1371/journal.pone.0031612.g001

$V_s = 0.02$ is small-vessel blood volume (including capillaries and small postcapillaries). V_l is blood volume of large blood vessels (veins and venules). It is associated with draining veins, and spatially varies across different brain areas in general. In this study we made use of high-resolution time-of-flight magnetic resonance angiography (TOF-MRA) scanning to accurately locate the blood vessels in the brain. The principle of TOF-MRA imaging is based on the enhancement of the signal of dynamic blood flow and the suppression of the signal of static tissues. The resolution of the TOF-MRA image was $0.9375 \times 0.9375 \times 1.5 mm^3$ (intensity range [0,1425]), which was much better than that of the fMRI image ($3.75 \times 3.75 \times 6 mm^3$, in this study). All images were collected in the same field of view (FOV). In TOF, veins usually bear higher signal intensities than the surrounding tissues, thus making the segmentation of major veins feasible and reliable. It is practicable to downsample the fine vasculature information to coarse fMRI scale in order to obtain the estimation of regional V_l at given fMRI voxels. We therefore attempted to combine the MR angiography image and the fMRI image for uncertainty reduction in data assimilation.

SPM2 program (Wellcome Department of Cognitive Neurology, http://www.fil.ion.ucl.ac.uk/spm) was used for our data pre-processing, voxel by voxel. Each fMRI volume was realigned to the first volume, and created a mean of the realigned data. The mean functional image then was upsampled to the resolution of the MRA. The MRA image was coregistered (Estimation and Reslice in SPM software) to the resultant upsampled mean image with linear interpolation. For high SNR TOF images, we performed the segmentation by simple thresholding. In the experiment, the segmentation threshold was set to 300 by simple visual guidance. After the vascular segmentation, we can obtain the large blood vessel composition (i.e. V_l) of each voxel in EPI images. Moreover, an isolated voxel with intensity higher than 300 was considered as noise and was therefore excluded from the calculation of V_0. Since the MRA image has a much higher spatial resolution than fMRI image (64 : 1 in this study), the large vessel fraction V_l of each voxel was expressed as:

$$V_l = \frac{\text{the number of MRA voxel occupied by vessels}}{\text{total MRA voxel number in a fMRI voxel}} = \frac{\text{the number of MRA voxel occupied by vessels}}{64} \quad (4)$$

Combined with the small-vessel fraction V_s, the total blood volume fraction of each voxel in fMRI image was expressed:

$$V_0 = V_l + V_s(1 - V_l) = V_l + 0.02(1 - V_l). \quad (5)$$

The first term represents the volume of blood from large vessels in a voxel, the second term is the blood volume fraction in the remaining brain tissue. In this sense, MRA can be thought of as an indirect, physical measurement of V_0, and can be treated as 'true' V_0 value. $V_0 = 0.02$ is a special case of the formulation when large vessel does not exist in this voxel.

Experiment and Data Preprocessing

The participant provided written informed consent before beginning the experiment which was approved by the Health Sciences Research Ethics Committee of Zhejiang University. Functional images were acquired on a 1.5-Tesla scanner (Marconi EDGE ECLIPSE) using a standard fMRI gradient echo echo-planar imaging (EPI) protocol (TE, 40 ms; TR, 2000 ms; flip angle, 90°; NEX, 1; FOV, 24 cm; resolution, 64×64 matrix). Sixteen contiguous 6-mm-thick slices, 0.5-mm-intervals were acquired to provide a coverage of the entire brain. Foam padding was used to limit head motion within the coil.

Before functional imaging, a high-resolution, three dimensional, spoiled gradient recalled at steady state anatomic image was collected (TE, 12 ms; TR, 500 ms; flip angle, 90°; NEX, 1; slice thickness, 6 mm; gap, 0.5 mm; FOV, 24 cm; resolution, 256×256 matrix) for anatomic localization and co-registration. Furthermore, a high-resolution angiography image was also collected for segmentation (TE, 7.47 ms; TR, 26 ms; flip angle, 60°; NEX, 0; slice thickness, 1.5 mm; FOV, 24 cm; resolution, 256×256 matrix).

Block design experiment was performed in this study. The subject was presented with classical flashing checkerboard pattern when scans were acquired. Activation maps ($P < 0.01$) were generated with the SPM software package (Wellcome Department of Cognitive Neurology, http://www.fil.ion.ucl.ac.uk/spm), which used a General Linear Model approach to detect regions with significant response during the task.

The Time-Of-Flight MR Angiography (TOF) image was segmented to extract the major veins in the brain. In TOF, veins usually bear higher signal intensities than the surrounding tissues, which makes the segmentation of major veins easy. For the high signal-noise-ratio (SNR) TOF images, we performed the segmentation by simple thresholding. The selection of threshold could be accomplished manually. In our work, we segmented veins by thresholding because of the high quality of the TOF image. Figure 2 presents an example of CBV imaging segmented from one subject. After thresholding, a de-noise step such as an opening operation, could be executed in order to eliminate some isolated noises. Once the segmented vasculature was obtained, we need to further transfer the information of vein position to the fMRI data. This requires that we registered/aligned the TOF to the fMRI image. Since the subject of the two images was the same patient in a short period, multi-modal rigid registration was enough to perform the task. We chose the classic mutual information as the similarity metric to do the 3D registration in the physical domain.

After finishing the segmentation and registration, we obtained corresponding brain blood volume in the voxel. The actual V_0 was then augmented into existing assimilation schemes [8,11,24]. In this study, two ROIs were selected from the greatest activation locus of primary visual cortex (V1) and V4 (Figure 3). We defined the clusters based on edges, but not included corners, so that the voxel had 4 neighbors (in the same slice). Figure 3 clearly shows

Figure 2. The vasculature of one subject.
doi:10.1371/journal.pone.0031612.g002
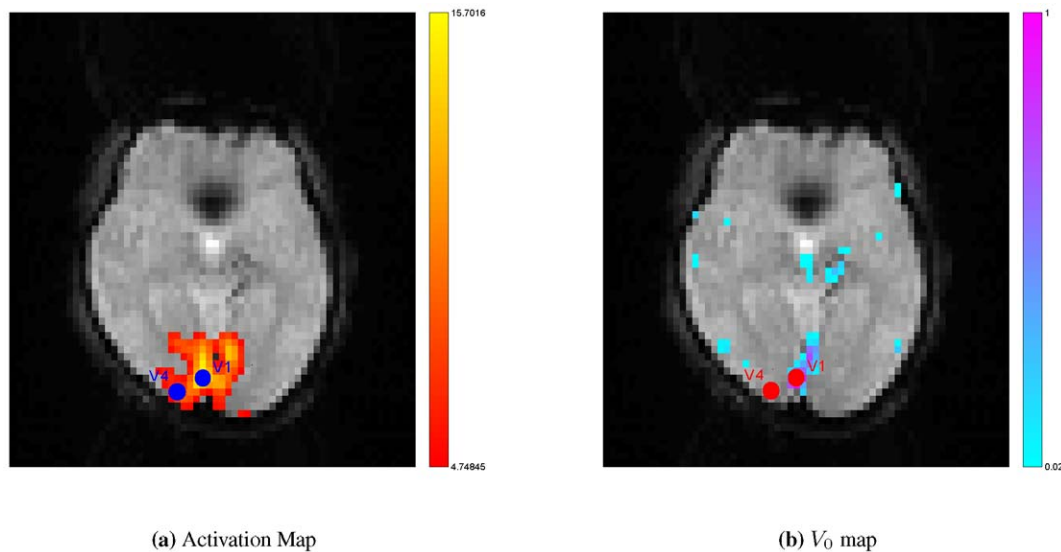
(a) Activation Map

(b) V_0 map

Figure 3. Regions of interest. Because BOLD contrast is highly weighted by venous blood content, activation areas often overlap with large vein regions. Two regions of interest (ROIs) were selected from visual cortex according to activation detection (warm color) and vascular information (cool color). The spatial resolution of venography map was downsample to identical with that of fMRI image. ($V1$: Primary visual cortex; $V4$: Visual area 4).
doi:10.1371/journal.pone.0031612.g003

that the activation area always overlap with the regions of large blood content. The spread activation along large veins in response to experimental stimulus could be observed. Actual V_0 was equal to 0.4947 in V1 locus due to the presence of large veins (Figure 3, right), and V_0 was still 0.02 in V4 locus because of the absence of large veins. The final time series were extracted by averaging the time series of 5 voxels.

Results

The Impact of V_0 on Single-region Data Assimilation

In this study, as a demonstration, we chose V1 as region of interest. We estimated the state functions and model parameters (Figure 3). Since there are not large veins in V4 area, this approach makes no difference in this area. For the sake of simplicity, we assumed a constant neural parameter $\epsilon_1 = \epsilon_2 = \cdots = \epsilon_n$ through-

out all trials, where n denotes trial number. The estimation scheme is formally identical to that in [24–26].

Figure 4 shows reconstructed BOLD response (left) and underlying physiological states (right) in the greatest activation locus of primary visual cortex (Figure 3) with actual V_0, given as solid line. As a comparison, we also evaluated the estimated BOLD response and physiological states with assumed $V_0 = 0.02$ value, which was widely employed in previous studies [3–8,10–16,18], given as dash line in Figure 4. We found that two different V_0 values produced very similar BOLD estimates (Figure 4, left), only tiny discrepancy in post stimulus undershoot stage could be found. Nevertheless, a significant distinction was observed in reconstructed physiological states between two values (Figure 4, right). Though the experimental stimulus induced a puny change in the blood flow f, the blood venous volume v and the veins dHb content q, the approach used assumed V_0 deduced a substantial
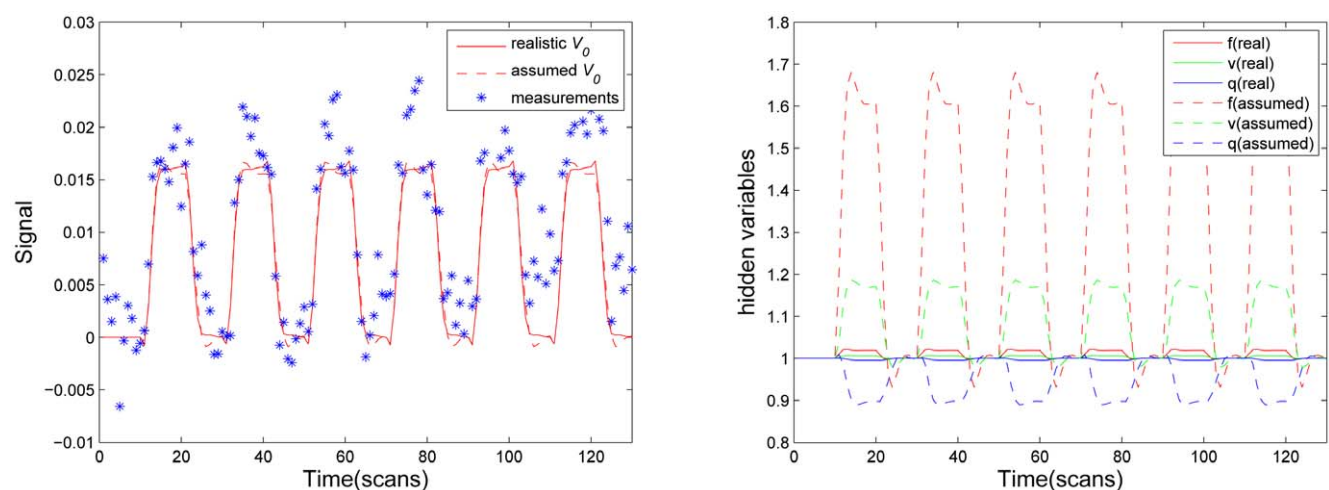

Figure 4. Estimated BOLD signal (Left), and reconstructed physiological states (Right) from the greatest activated locus in primary visual cortex (V1). For comparative purpose, model estimation was also performed with a typical assumed $V_0 = 0.02$. Real V_0 value is 0.4947.
doi:10.1371/journal.pone.0031612.g004

change during task due to magnifying effect of large blood content. This implied that the presence of large veins in an activated area contributed excess signal in this area. The change of BOLD signal in this area mainly derived from the large-vessel signal, not from the multiple physiological states, namely, not from the experimental related neuronal activity. Since statistical inference essentially is grounded on the amplitude of BOLD response, this area may surely be considered active in statistic analysis of the BOLD signal change, though it is absent at the response efficacy elicited by neuronal activity. This explains why the employment of assumed V_0 in detection process still could generate very similar activation map with those obtained from classic linear model [10,11]. The same difference also can be found in estimated model parameters (Table 1). Specially, neuronal efficacy ϵ is 0.0094 with actual V_0 derived from MRA image, while ϵ is 0.1534 with assumed V_0 value. Assumed, underestimated V_0 substantially overestimates the neuronal efficacy parameter, ϵ. Since parameter ϵ reflects the efficacy with which neuronal activity causes an increase in signal, we argue that the estimated efficiency parameter ϵ in each voxel might be a good index to sign actual activation level.

The Impact of V_0 on Dynamic Causal Models (DCM)

Dynamic causal modeling (DCM) has been introduced as a generic method to explore effective connectivity from the hemodynamic observations [12,27]. Apart from Balloon model, this model additionally embeds a neurobiological modelization of the dynamic interactions among brain areas into the hemodynamic models in these areas, and it can be regarded as an extension of hemodynamic model from single region to covering multiple regions. Single-region data assimilation supposes that extrinsic experimental input consistently accesses all brain regions, whereas DCM designs that inputs produce responses in two different ways: extrinsic influence from sensory input and intrinsic influence from interaction regions. As uncertain V_0 makes the greatest impact on estimates of neuronal efficacy parameter ϵ in hemodynamic model, it is interesting to investigate the effect of V_0 on DCM.

In this study, as an example, two regions were selected using maxima of activation map to construct the hierarchical system. The system architecture was shown in Figure 5. The two maxima were located in visual area V1 and V4. Region-specific time series comprised all neighbor voxels of each maxima location (a total of 5 voxels). The location is shown in Figure 3. The system describes a simple hierarchy of forward connections where two primary motor regions influence each other, and can be expressed as the following

$$\dot{x}_1 = a_{11}x_1 + a_{12}x_2 + c_{11}u_1 \tag{6}$$

$$\dot{x}_2 = a_{22}x_2 + a_{21}x_1 + c_{22}u_2 \tag{7}$$

where $x_1(x_2)$ is neuronal dynamics in V1 (V4); u_1 and u_2 represent external inputs into the system; $a_{11}(a_{22})$ represents the inner connectivity within the region in the absence of input; $a_{12}(a_{21})$ encodes the fixed inter-regions connectivity in the absence of input; $c_{11}(c_{22})$ embodies the extrinsic influences of input on neuronal activity.

Equations (6) and (7) then were appended into the states vector [8,11]. The measurement vector was expanded to include two observations in the two areas as well. Two inputs corresponded to a $0-1$ quarewave function for the occurrence of experimental stimulus (Figure 5). The outputs of the system are two time series from two regions. The estimation scheme employed for DCM is formally identical to that in previous studies [8,11].

The results of this analysis are presented in Figure 5. The connections are shown as directed black arrows with the coupling parameters calculated with actual V_0 alongside. The values in brackets are parameters estimated with assumed V_0. $V_0 = 0.4947$ in visual area V1, $V_0 = 0.02$ in V4 and assumed $V_0 = 0.02$ in two areas. As expected, the significant difference in connectivity parameters with actual V_0 and assumed V_0 can be found (Figure 5). The fixed connectivity from V1(V4) to V4(V1) is -0.28 while considering the contribution of vessels, whereas the value is -0.50 while the effect was discounted.

From the above analysis, the employment of an assumed V_0 in the hemodynamic data assimilation seems to be only suitable for fMRI signal reconstruction and activation detection grounded on this estimated signal, not for effective connectivity study that by means of estimated neuronal activity (e.g. $\epsilon u(t)$) makes inference about the coupling among brain areas and how that coupling is influenced by changes in experimental context. Due to the regulation of resting blood volume fraction (V_0), in fMRI imaging, large BOLD signal changes are often associated with large draining veins, while tissue areas have low BOLD signal changes. These results suggest that the impact of V_0 on fMRI data assimilation should be considered. Actual V_0 should be investigated or these areas that are dominated by large veins should be excluded in the region-specific analysis.

Discussion

This work is principally concerned with an important but long ignored issue in previous efforts on the hemodynamic model – the influence of resting cerebral blood volume fraction V_0. Previous studies postulated a physiologically plausible value $V_0 = 0.02$ in assimilation procedure to handle ill-posedness of the problem, as opposed to exploring true BVF. This practice may lead to inaccurate results. In this study, instead of arbitrary assignment, we propose a combinative approach that supplements realistic V_0 derived from MR angiography (MRA) image into an existing hemodynamic assimilation scheme to achieve more reliable model estimation. We find that V_0 has a complicated influence on assimilation results. Though arbitrarily assigned V_0 can produce similar BOLD response with realistic V_0, there is significant difference in reconstructed physiological states and estimated model parameters, indicating that the application of these parameter estimated by assumed V_0 should be justified and interpreted with caution [7,28]. Moreover, as uncertain V_0 value leads to larger deviation in estimated efficacy parameters ϵ than that in other parameters, we also have investigated the influence of V_0 on dynamic causality modeling which estimates connectivity in different brain regions by means of ϵ estimates. Not surprisingly,

Table 1. Estimated model parameters with true value (V_t) and typical assumed value (V_a) in the greatest activated locus of primary visual cortex (V1).

V_0	Model Parameters				
	ϵ	τ_s	τ_f	τ_0	E_0
$V_t = 0.4947$	0.0094	1.3635	2.0346	2.5204	0.6716
$V_a = 0.02$	0.1534	1.7576	3.9874	2.0137	0.7424

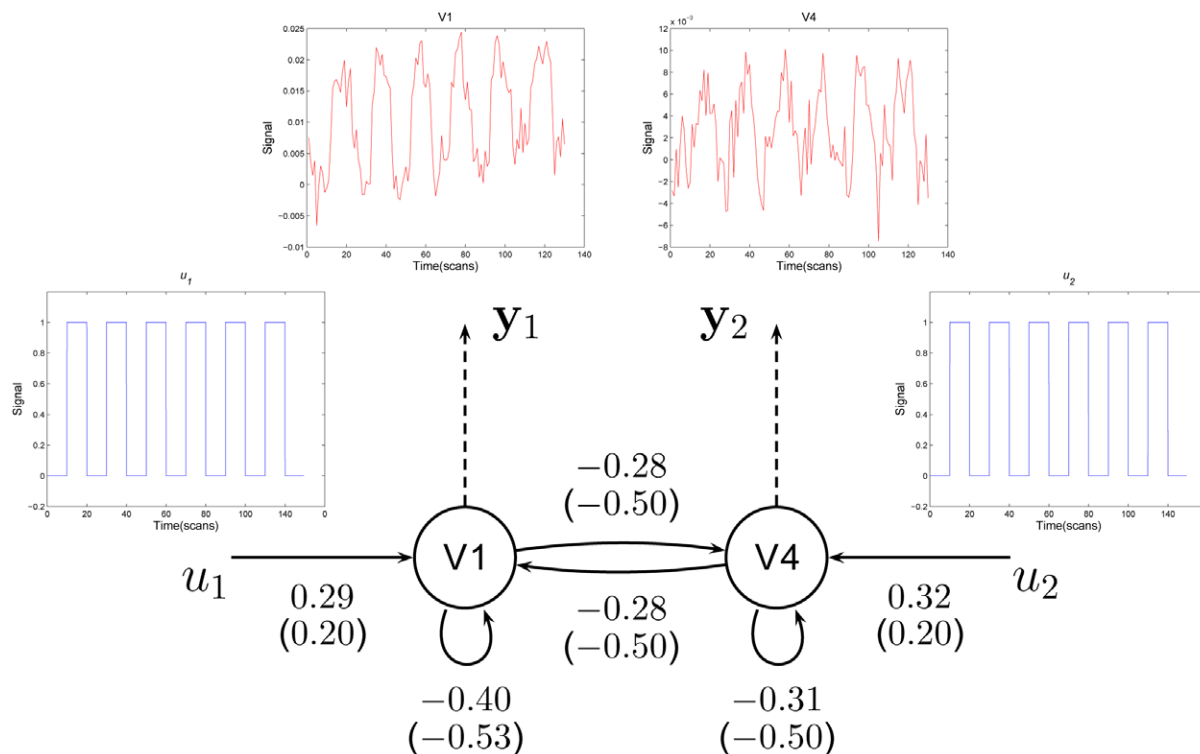doi:10.1371/journal.pone.0031612.t001

Figure 5. Results of a two-node DCM analysis applied to the flashing checkerboard experiment. The coupling parameters calculated with actual V_0 are shown alongside the corresponding connections. The values in brackets are parameters estimated with assumed V_0. $V_0 = 0.4947$ in visual area V1, $V_0 = 0.02$ in V4 and assumed $V_0 = 0.02$ in two areas. u_1 and u_2 represent external inputs into the system; y_1 and y_2 are the hemodynamic observations and arrows indicate connections.
doi:10.1371/journal.pone.0031612.g005

V_0 has also considerable impact on the evaluation of brain connectivity. We thereby argue that introducing more realistic V_0 in DCM can provide more reliable estimation of interregional coupling, and assist to acquire a better understanding of brain connectivity that is of considerable interest in neuroimage community recently, such as Human Connectome Project (HCP) in NIH, Brain CONNECT Project in Europe, and National Basic Research Program of China (973) under Grant 2011CB707800.

A possible criticism on this work is to what extent MRA image is able to provide accurate actual cerebral blood volume fraction reflecting BOLD response. Indeed MRA imaging is not a direct, physical measurement of V_0. However, as noted, the MRA image has a much higher spatial resolution than a fMRI image (64 : 1 in this study). In this sense, MRA can be thought of as an indirect, physical measurement of large veins component V_l in given areas. Combining with tissue blood volume component V_s, a more realistic V_0 value can be obtained. An imperfect measurement is better than arbitrary assignment without any measurement. As more physical realistic V_0 is incorporated into the assimilation procedure, more reliable information of the underlying physiological dynamics is reconstructed, and physiologically more meaningful results may be expected. Another limitation is that few experiments were performed in this study. The main cause is the incorrect but pervasive belief that MRI scans are harmful to health in China. The recruitment of subjects was very difficult. This was even reported recently by Nature [29]. However, our study is mainly concerned with the influence of V_0 on assimilation, and to discuss the importance of introducing actual V_0 information into the assimilation process. The results clearly illustrate our intention. We therefore believe that more experiments is not necessary. Despite these limitations, we argue that such a effort is valuable and should be well appreciated, in particular, while nearly 400 studies on hemodynamic data assimilation have been reported every year [30]. Currently, we are trying to experimentally verify that augmenting more realistic V_0 derived from MRA imaging into assimilation process will provide more accurate states forecast and parameter estimation.

Author Contributions

Conceived and designed the experiments: ZH. Performed the experiments: ZH HL. Analyzed the data: ZH CL. Contributed reagents/materials/analysis tools: ZH PS. Wrote the paper: ZH.

References

1. Buxton RB, Wong EC, Frank LR (1998) Dynamics of Blood Flow and Oxygenation Changes During Brain Activation: The Balloon Model. Magnetic Resonance in Medicine 39: 855–864.

2. Buxton RB, Frank LR (1997) A model for the coupling between cerebral blood flow and oxygen metabolism during neural stimulation. Journal of Cerebral Blood & Flow Metabolism 17: 64–72.

3. Friston KJ, Mechelli A, Turner R, Price CJ (2000) Nonlinear Responses in fMRI: The Balloon Model, Volterra Kernels, and Other Hemodynamics. NeuroImage 12: 466–477.

4. Riera JJ, Watanabe J, Kazuki I, Naoki M, Aubert E, et al. (2004) A State-space Model of the Hemodynamic Approach: Nonlinear Filtering of BOLD Signals. NeuroImage 21: 547–567.

5. Johnston LA, Duff E, Egan GF (2006) Particle Filtering for Nonlinear BOLD Signal Analysis. In: 9th International Conference on Medical Image Computing and Computer Assisted Intervention (MICCAI). Copenhagen, Denmark. pp 292–299.

6. Hu ZH, Zhang HY, Wang LW, Song XL, Shi PC (2007) Joint Estimation for Nonlinear Dynamic System from fMRI Time Series. In: 14th IEEE International Conference on Image Processing (ICIP). San Antonio, TX, USA, . pp 145–148.

7. Johnston LA, Duff E, Mareels I, Egan GF (2008) Nonlinear Estimation of the BOLD signal. NeuroImage 40: 504–514.

8. Hu ZH, Zhao XH, Liu HF, Shi PC (2009) Nonlinear Analysis of the BOLD signal. EURASIP Journal on Advances in Signal Processing 2009: 1–13.

9. Hettiarachchi IT, Pathirana PN, Brotchie P (2010) A State Space Based Approach in Non-Linear Hemodynamic Response Modeling with fMRI Data. In: 32nd Annual International Conference of the IEEE EMBS. Buenos Aires, Argentina. pp 2391–2394.

10. Deneux T, Faugeras O (2006) Using Nonlinear Models in fMRI Data Analysis: Model Selection and Activation Detection. NeuroImage 32: 1669–1689.

11. Hu ZH, Shi PC (2007) Nonlinear Analysis of BOLD Signal: Biophysical Modeling, Physiological States, and Functional Activation. In: 10th International Conference on Medical Image Computing and Computer Assisted Intervention (MICCAI). Brisbane, Australia. pp 734–741.

12. Friston KJ, Harrison L, Penny W (2003) Dynamic Causal Modeling. NeuroImage 19: 1273–1302.

13. Mechelli A, Price CJ, Noppeney U, Friston KJ (2003) A Dynamic Causal Modeling Study on category effects: bottom-up or top-down mediation? Journal of Cognitive Neuroscience 15: 925–934.

14. Penny WD, Stephan KE, Mechelli A, Friston KJ (2004) Comparing Dynamic Causal Models. NeuroImage 22: 1157–1172.

15. Friston KJ, Trujillo-Barreto N, Daunizeau J (2008) DEM: A Variational Treatment of Dynamic Systems. NeuroImage 41: 849–885.

16. Li XF, Marrelec G, Hess RF, Benali H (2010) A Nonlinear Identification Method to Study Effective Connectivity in Functional MRI. Medical Image Analysis 14(1): 30–38.

17. Hu ZH, Shi PC (2010) Sensitivity Analysis for Biomedical Models. IEEE Transaction on Medical Image 29: 1870–1881.

18. Friston KJ (2002) Nonlinear Responses in fMRI: Bayesian Estimation of Dynamical Systems: An Application to fMRI. NeuroImage 16: 513–530.

19. Jezzard P, Matthews PM, Smith SM (2001) Functional MRI: An Introduction to Methods. New York: Oxford University Press.

20. Lu HZ, Law M, Johnson G, Ge Y, van Zijl PC, Helpern JA (2005) Novel Approach to the Measurement of Absolute Cerebral Blood Volume Using Vascular-Space-Occupancy Magnetic Resonance Imaging. Magnetic Resonance in Medicine 54: 1403–1411.

21. Zheng Y, Martindale J, Johnston D, Jones M, Berwick J, et al. (2002) A Model of the Hemodynamic Response and Oxygen Delivery to Brain. NeuroImage 16: 617–637.

22. Buxton RB, Uludağ K, Dubowitz DJ, Liu TT (2004) Modeling the Hemodynamic Response to Brain Activation. NeuroImage 23: S220–S233.

23. Zheng Y, Johnston D, Berwick J, Chen D, Billings S, et al. (2005) A Three-compartment Model of the Hemodynamic Response and Oxygen Delivery to Brain. NeuroImage 28: 925–939.

24. Hu ZH, Fang X, Shen XY, Shi PC (2009) Exploiting MR Venography Segmentation for the Accurate Model Estimation of BOLD Signal. In: 2009 IEEE International Symposium on Biomedical Imaging: From Nano to Macro (ISBI). Boston, MA, USA. pp 706–709.

25. Tsoulos IG, Lagaris IE (2006) Genetically Controlled Random Search: A Global Optimization Method for Continuous Multidimensional Functions. Computer Physics Communications 174: 152–159.

26. Ali MM, Törn A, Viitanen S (1997) A Numerical Comparison of Some Modified Controlled Random Search Algorithms. Journal of Global Optimization 11: 377–385.

27. Stephan KE, Kasper L, Harrison LM, Daunizeau J, den Ouden HEM, et al. (2008) Nonlinear Dynamic Causal Models for fMRI. NeuroImage 42: 649–662.

28. David O, Guillemain I, Saillet S, Reyt S, Deransart C, et al. (2008) Identifying Neural Drivers with Functional MRI: An Electrophysiological Validation. PLoS Biology 6: 2683–2697.

29. Jiao L (2010) Fear of MRI trips up brain Researchers. Nature 327: 931.

30. Friston KJ (2009) Causal Modelling and Brain Connectivity in Functional Magnetic Resonance Imaging. PLoS Biology 7: 220–225.